

Information Value Based Spatio-Statistical Modelling for Landslide Vulnerability Mapping, the Nilgiris, Western Ghats, South India

SM Ramasamy^{1,*}, M Muthukumar²

¹Department of Remote sensing, Bharathidasan University, Tiruchirappalli-620 023, India

²Centre for Geoinformatics, Gandhigram Rural University, Dindigul, Tamilnadu-624 302, India

Corresponding Author: SM Ramasamy, Department of Remote sensing, Bharathidasan University, Tiruchirappalli-620 023, India, Tel.: 09443352543, E-mail: smrsamy@gmail.com

Citation: SM Ramasamy, M Muthukumar (2024) Information Value Based Spatio-Statistical Modelling for Landslide Vulnerability Mapping, the Nilgiris, Western Ghats, South India, Int J Eng Geol Environ 1: 1-16

Copyright: © 2024 SM Ramasamy. This is an open-access article distributed under the terms of Creative Commons Attribution License, which permits unrestricted use, distribution, and reproduction in any medium, provided the original author and source are credited.

Abstract

Since the landslides were once thought to be confined to the younger and tectonically active mountain belts, the Geoscientists were attributing it mostly to active and seismo-tectonics and hence have been focusing more on them. But later on, when the landslides started occurring in the other mountain systems also, they were stimulated to think that, besides the active-seismo-tectonics and the ages of the mountains, the other geological parameters, triggering parameters like rainfall and the anthropogenic activities can also cause landslides. So, studies were started in multiple directions, in different mountain ranges around the world. But these studies were mostly involved with the preparation and integration of various thematic maps connected to the geosystems and the other parameters related to landslides. In this process, different workers used various combinations of input parameter maps with differing resolutions, different ways of assigning landslide vulnerability weightages and also various methods of integrating them to prepare landslide vulnerability maps. These resulted into outputs of varying landslide vulnerabilities and reliabilities. However, in this, the bias of the individuals also had its own role. So, in the present study, the information value (IFV) based spatio-statistical method was carried out for a test site in Nilgiris mountains, Western Ghats, South India involving all the possible geosystem variables/parameters. In this method, discrete Information Value based weightages were assigned to the different sub variables of each of the main geosystem variables on the basis of number of landslides falling in each sub variable and computing the weightages using the formula $[(S_i / N_i) / (S/N)]$ developed and demonstrated by Yin and Yan (1988). Then the final GIS based integration of all the weighted geosystem variables was done which led to the precise landslide vulnerability map for the study area.

Keywords: Landslide Vulnerability Mapping; Information Value Method In Landslides; GIS; Nilgiris Mountains; South India

Introduction

Due to the higher frequency and the magnitude of the Landslides mostly in the tectonically active and younger mountain belts of the world, the geoscientists have all along been having strong conviction that only these types of mountains are vulnerable to landslides. So, they have focused more in studying the younger and active mountains around the world [1-8]. But later, since the other mountain ranges have also started witnessing landslides irrespective of their tectonic vulnerabilities and the ages, the scientists were provoked to think that the geosystem parameters/variables other than the active tectonics and the ages of the mountains can also cause landslides. So, they have started studying the other older and the tectonically stable mountain regions too using various geosystem parameters/variables and the other landslide related variables. These studies led to the inference that both individually or in different combinations these landslide related parameters can also cause landslides [9-18]. Further, in these studies, mostly the spatial data bases were prepared on different geosystem parameters/variables, triggering parameters and the anthropogenic variables and integrated them using the advanced virtues available with remote sensing, GIS, statistics and Information Technology tools, to bring out the landslide vulnerability maps [19-24]. But in these studies, different researchers have used (i) various combinations of Geosystem parameters and the other parameters /variables related to landslides, (ii) maps of different spatial resolutions, (iii) different norms of assigning weightages to the variables and (iv) different methods of spatial integration. These have yielded Landslide Vulnerability Maps (LVM) of differing standards, precision, and reliabilities. Hence, after detailed browsing of the earlier studies, spatial data bases were generated on different types of landslide related parameters viz. Rock types, tectonic features, degree of weathering, slope morphometry, geomorphology, Land use/Land cover; the triggering parameters like drainage triggered toe removal along the toes of the slopes and the other anthropogenic activities like road cutting along the slopes and the toes, removal of vegetation and the other similar variables, and the spatio-statistical analysis was carried out using the Information value (IFV) based method to prepare the Landslide Vulnerability map, evaluate its efficiency and to suggest for its replication in other parts of the world. This was done by selecting 300 sq.km area in parts of The Nilgiris mountains, which is one of the major mountain belts of India belonging to the Western Ghats, where landslides occur frequently [9] (Figure 1).

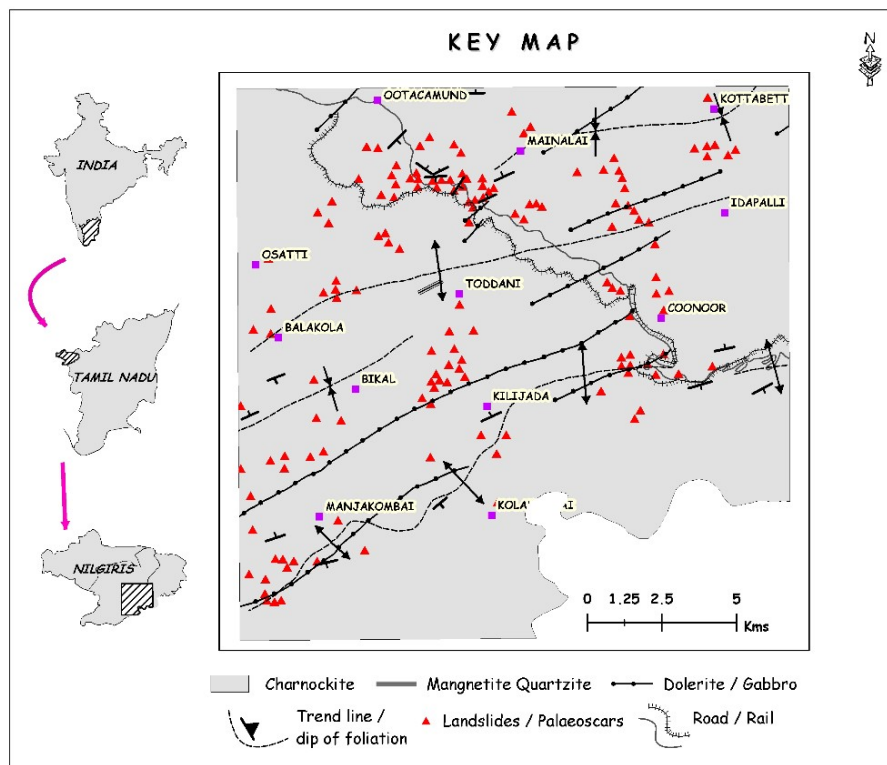


FIG. 1. Study area Geology - Landslides Distribution

Figure 1: Key Map and Landslides

Methodology in Brief (Figure 2)

In the said study, the GIS database was generated using Arc-GIS on the distribution of Landslides from the interpretation of aerial photographs and satellite multi-spectral data, collection of collateral data and field inventory (Fig.1). Similarly, GIS databases were generated on 12 geosystem variables related to landslides viz.(i) lithology, (ii)lineament frequency, (iii)lineament density, (iv) lineament intersection density, (v) Azimuthal Relation between the topographic ridges & Joints,(vi) angular relation between the slope of the topographic ridges& dip of the joints (vii) dip of the joints, (viii) slope, (ix) geomorphology,(x) land use /cover, which includes the anthropogenic variables, (xi) regolith and (xii) drainage density. These 12 variables had number of sub variables/ classes in each of them. For example, the variable lithology, namely the Charnockite, was mapped into three sub variables namely the highly, moderately, and poorly weathered charnockites. Similarly, the other 11 variables were classified into a number sub variables depending upon their respective criteria. For example, for the geosystems like geomorphology and the land use /land cover (ix & x), the actual landforms in the case of geomorphology and the features in the case of Land use /Land cover were mapped and considered as sub variables. Where as in the case of variables like the three derivatives of the lineaments (ii, iii & iv), three major variables of topographic ridges and the joints(v, vi & vii), slope(viii) regolith (xi) and the drainage density (xii) were mapped/classified into five numbers of sub variables based on the dynamic range of their values .

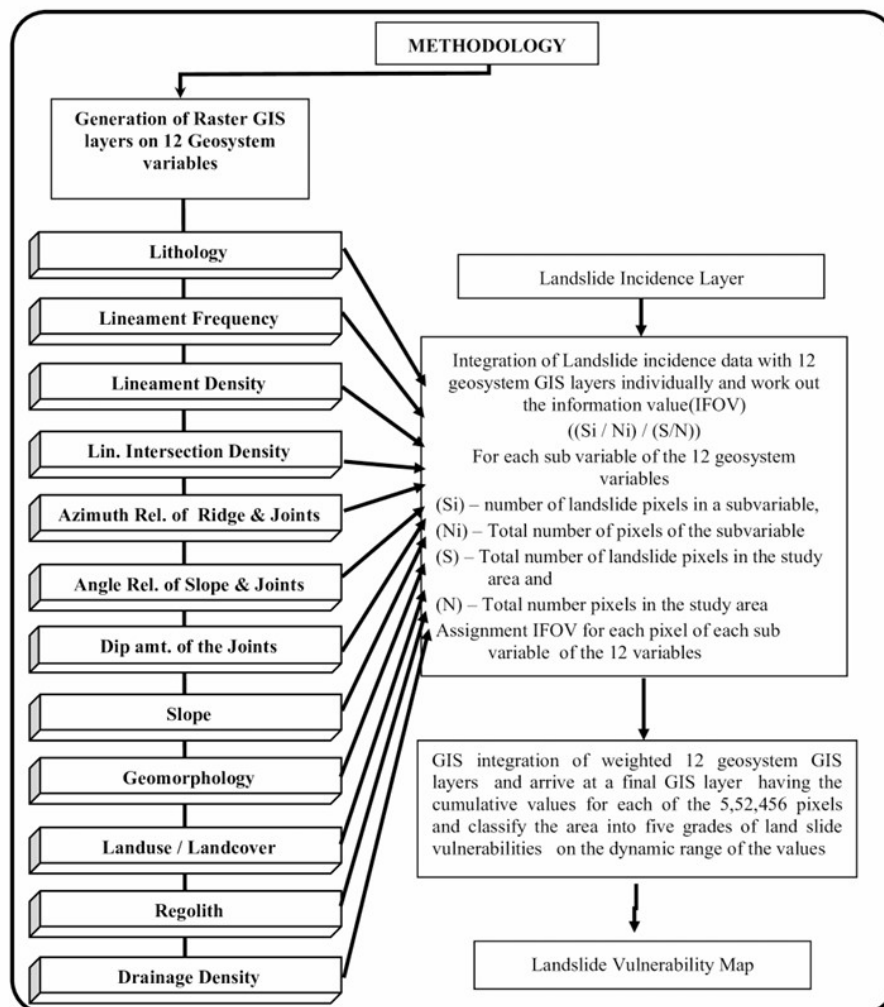


Figure 2: Methodology

Then, these 12 vector based GIS geosystem variables of the entire study area of 300 sq.km were individually converted into 12 raster GIS data bases with 5,52,456 number of pixels of 23.5m² each using the vector to raster conversion menu of ARC-GIS. Then, the information values were worked out for each of the sub variables of the 12 geosystem variables using the formula $[\log (Si/Ni) / (S/N)]$ developed by Yin and Yan²⁷. In this formula 'Si' is the number of landslide pixels in a particular sub variable,

'Ni' is the total number of pixels of the same sub variable, 'S' is the total number of landslide pixels in the study area of 300 sq.km and the 'N' is the total number of pixels of the study area of again 300 sq.km. After working out the information values for each sub variable, those values were assigned to each pixel of the respective sub variables. Then all the 12-raster based weighted geo system variables having a number of weighted sub variables in them were integrated using ADD function menu of ARC GIS and cumulative information values of each of the 5,52,456 pixels were arrived for the study area. Finally, from the dynamic range of the total information values of the 5,52,456 pixels, the study area was grouped into five zones as very high, high, moderate, low and very low zones of landslide vulnerabilities. In the study, the anthropogenic variables automatically figured in the land use/land cover variable; whereas the rainfall has not been given separate status as a variable, because it is the triggering parameter and as when it interferes with the terrain, the terrain systems will respond differentially and cause landslides according to their vulnerability grades arrived from the Information Values.

Generation of Gis Data Bases on Landslides

In the said study, Black & white panchromatic aerial photographs of 1:10,000 scale were studied under stereo model and Landslides, which showed distinct morphological features in the form of well-defined crown, slip planes, traces of sliding, accumulation of such slided materials forming toes, talus etc. were mapped. The landslides were also mapped from the digitally processed IRS P 6 LISS III data, which vividly displayed the vegetation blanks reflecting the Landslide geometries. In addition, the data on the palaeo scars brought out by the earlier workers⁹ was also incorporated. With these basic inputs, the detailed field inventory was made and finally overall 300 landslides and palaeo scars were located. Out of these, 144 landslides of appreciable size were filtered out and GIS database was generated showing the distribution of such landslides using the ARC -GIS software (Figure 1). In fact in the entire analyses, as far as GIS is concerned, either for generating the spatial data bases or for the integration of various spatial data bases, ARC -GIS only was used.

Generation of Gis Databases on Geosystems

Similarly, GIS databases were generated for the above said 12 landslide related Geosystem variables

Lithology

Detailed interpretation was made on the lithology of the study area using the enlarged formats of the raw and the digitally processed IRS P -6 Resource satellite data. The study revealed that the study area was completely covered only by Charnockites of the Peninsular Gneissic Complex of Archaean-Proterozoic Era. However based on the tonal, textural, vegetation, drainage and the land use /land cover characteristics, the Charnockite was classified into three sub variables viz. highly, moderately and poorly weathered Charnockites; these were also field checked and confirmed.

The lithology map thus prepared with three sub variables for the entire study area was digitized and vector-based GIS data base was generated and, later converted into raster GIS data having total number of 5,52,456 pixels of 23.5m² each for the study area (Figure 3A). In this, the highly weathered, the moderately weathered and the poorly weathered Charnockites respectively covered 2,17,983 pixels, 2,07,817 pixels and 1,26,656 pixels in the total study area of 5,42,456 pixels (Figure 3A).

Lineament Frequency

From the IRS P6 FCC data, all the lineaments of tectonic origin were interpreted using various photo recognition elements like tonal, textural, topographical, soil tonal and structural and vegetation linearities and curvilinearities [28]. From the Lineament map, lineament frequency map was prepared by counting the total number of lineaments per each grid of 250m x 250m and contouring them [25]. Then, based on the dynamic range of the values of the contours, the lineament frequency was grouped into 5 classes/ sub variables, such as very high, High, Moderate, Low, and very low zones of lineament frequency. Such vector GIS based classified lineament frequency map was converted into Raster GIS data, in which the sub variables, namely the zones of very high frequency covered 2306 pixels, high frequency covered 30,231 pixels, moderate frequency covered 1,78,843 pixels,

low frequency occupied 2,95,008 pixels and the very low frequency covered 46,068 pixels (Fig. 3B) in the total area of 5,52,456 pixels of the study area .

Lineament Density

Similarly from the same lineament map , the vector GIS data was prepared on lineament density, by counting the total length of lineaments per 250x 250 m² grid and contouring them [25]. Based on the range of the lineament density values, the contours were grouped into 5 classes / sub variables as very high, High, moderate, low and very low zones of lineament density .

Such vector based GIS data on lineament density was converted into Raster GIS data and in it, the five sub variables of lineament density from very high to very low have respectively covered 69,170; 1,04,012; 1,75,025; 1,54,278 and 49,971 pixels of 250mx250m each (Figure 3C) in the study area of 5,52,456 pixels .

Lineament Intersection Density

Similarly, the vector GIS data on lineament intersection density was prepared, and in this case, the lineament intersections were counted per 250m x 250m grid and contoured²⁵. It was then similarly classified into five classes / variables of lineament intersection density on the basis of the range of the values of the contours and then converted into raster GIS data in which the five such classes of lineament intersection density viz. very high, high, moderate, low and very low have respectively covered 1858; 22,779; 2,94,585; 2,04,686 and 28,548 pixels of 250mx250m each (Figure 3D) in the study area of 5,52,456 pixels.

Azimuthal Relation Between Topographic Ridges and Joints

Due to the tectonic activities and the followed up erosion by the fluvial actions, the mountains have respectively developed joints and the topographic ridges , the later displaying well defined crest lines. The azimuthal relation between the crest lines of the topographic ridges and the strike of the joints forms one of the important factors in controlling landslides. For example, when the angle between the orientation of the crestlines of the topographic ridges and the strike of the joints are lesser and lesser, the landslide vulnerability will gradually increase and vice-versa. So, this has been taken as one of the important variables in landslide vulnerability mapping. Accordingly, the GIS database was generated on this. To do it, the study area was mapped into 695 number of slope facets based on the morphology of the topographic contours collected from the Survey of India topographic sheets on 1:25,000 scale. Then in each slope facet, the orientation of the crestline of the topographic/slope ridges was marked with the help of the toposheets and the field surveys and whereas the strike of the prominent joints were mapped by carrying out field surveys. Followingly , on the basis of the angular relation between the both, these 695 slope facets were classified into five classes viz; <5°, 5°- 10°, 10° - 20°, 20°-30° and > 30°. Then , such classified vector based slope facet data was converted into raster GIS data with slope facets falling in <5° class as very highly vulnerable to landslides , which covered 3,25,294 pixels, 5°- 10° as highly vulnerable which covered 76,359 pixels, 10° - 20° as moderately vulnerable which covered 93,712 pixels, 20°-30° as poorly vulnerable covering 20,085 pixels, and > 30° class of slope facets as very poorly vulnerable having 37,006 pixels (Figure 3E).

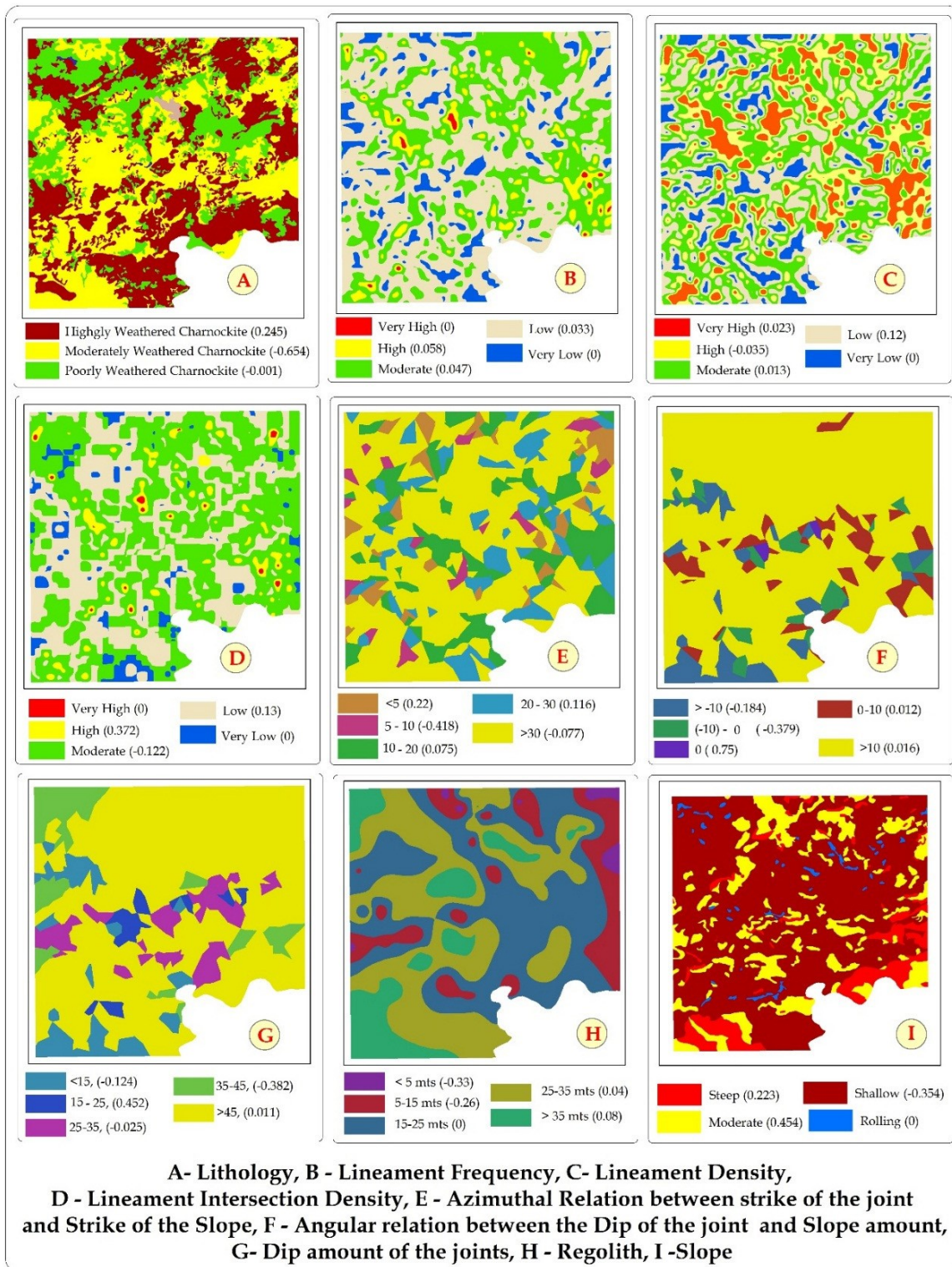


Figure 3: Information Value based Weighted Raster GIS data bases on Geosystems

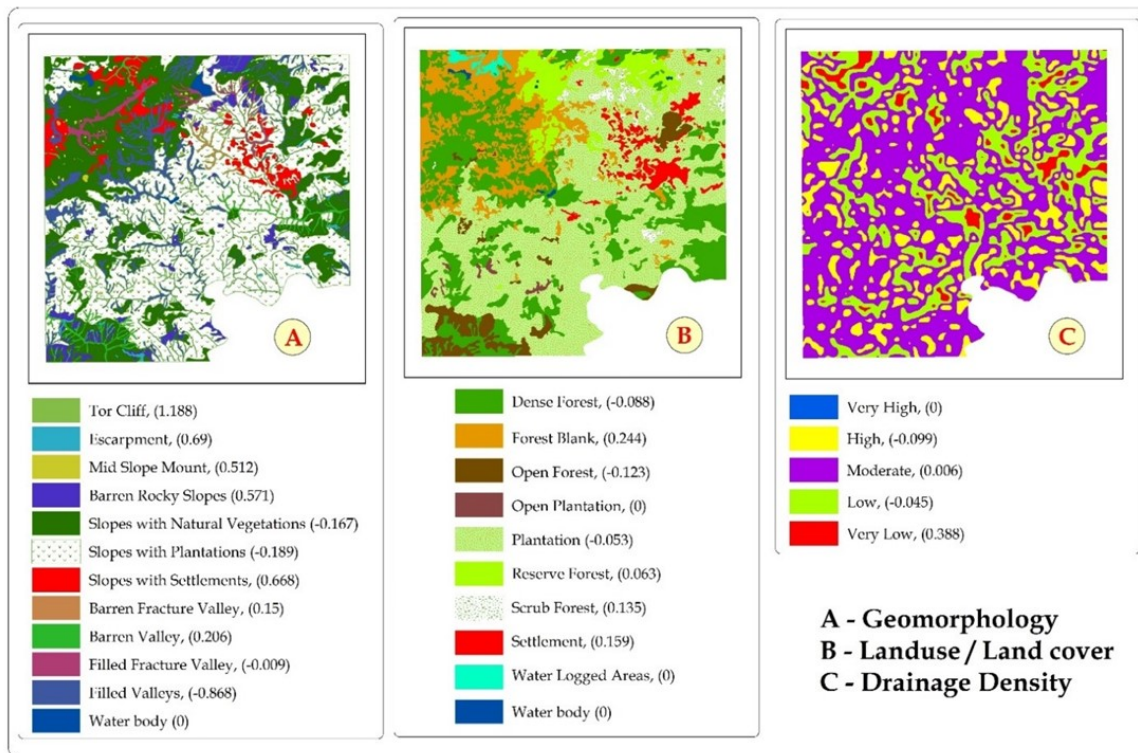


Figure 4: Information Value based Weighted Raster GIS layers on Geosystems

Angular Relation Between the Slope of the Topographic Ridges and Dip of Joints

If the dip of the joints and the slope of the topographic ridges are in the same direction that too with less angle between the both, then the landslide probabilities will be high. In contrast, if these are in opposite directions, then the landslide vulnerability is less. So, the facet wise vector GIS database was generated on this. In this, if both are in the same direction then negative signs were given for the angle between the dip of the joints and the slope of the topographic ridges. On the contrary, if both are in the opposite directions, then the angle between them were assigned positive signs. For example, if the slope of the topographic ridge was 40° towards northerly and the joint was also dipping 55° towards northerly, then the dip-slope relation was noted as -15° (Fig. 5A). Whereas, if the slope of the topographic ridge was 40° towards northerly and the dip of the joints was 55° towards southerly then the angle between the both was taken as $+95^\circ$ (Fig. 5B). Thus, such angular relation between the slope of the topographic ridge and the dip of the joints were worked out for all the 695 slope facets. Then depending upon the dip-slope relations, these 695 slope facets were grouped into five classes such as $> -10^\circ$, -10° to 0° , 0° , 0° to $+10^\circ$ and $> +10^\circ$. Then, such vector GIS slope facet data having these five classes of slope facets were rasterized into 5, 52, 456 pixels for the study area with the same pixel size of $23.5 \times 23.5 \text{ m}^2$ as was done for the other geosystem variables (Fig. 3F). In this these, the slope facet class with greater than -10° covered 4,36,366 pixels, -10° - 0° covered 44,798 pixels, 0° class covered 2730 pixels, 0° - 10° class covered 27,530 pixels and $> +10^\circ$ class covered 41,032 pixels in the total area of 5,52,456 pixels of the study area.

Dip Amount of Joints

Similarly, if the amount of dip of the joints is less, then the landslide probability will be high. So, on the basis of the dip amount of joints, the 695 slope facets were classified into five groups, such as slope facets with joints of $<15^\circ$ dip, $15^\circ - 25^\circ$, $25^\circ - 35^\circ$, $35^\circ - 45^\circ$ & $>45^\circ$. Such classified slope facet data was converted into raster GIS showing such five classes with cumulative 5,52,456 pixels of $23.5 \times 23.5 \text{ m}^2$ size each (Fig. 3G). In this the slope facets with the $<15^\circ$ dip class covered 40,873 pixels, $15^\circ - 25^\circ$ dip class covered 16,256 pixels, $25^\circ - 35^\circ$ dip class covered 44,727 pixels, $35^\circ - 45^\circ$ dip class covered 46,270 pixels & $>45^\circ$ dip class covered 4,04,330 pixels.

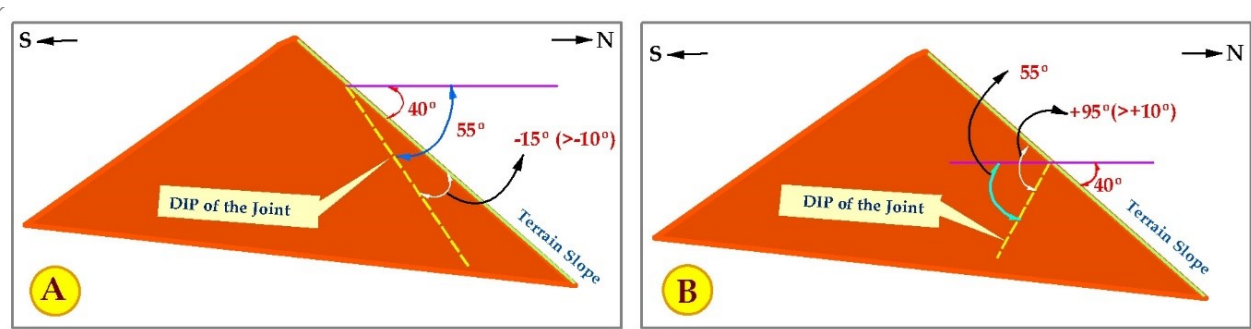


Figure 5: Angular Relation between Slope and Dip of Joints

Regolith

The landslide vulnerability is directly proportional to the degree of weathering. So, the GIS database was generated on the thickness of regolith. To do it, geophysical resistivity survey was conducted in 100 locations using Wenner Configuration up to a depth of 50 to 70 mts and using inverse slope method, thickness of topsoil, weathered zone and fractured zone and therefrom the cumulative thickness of regolith was worked out for these 100 locations. These were plotted in the respective locations and contoured. The same contour values varied from 0 to 55 mts. From these contours, the study area was grouped into 5 classes (< 5, 5-15, 15-25, 25-35 and > 35m thickness) .Such classified vector GIS data was rasterised with the pixel size of 23.5 x 23.5 m² and with the total number of pixels of 5,52,456 for the total study area matching with other geosystem variables (Fig. 3H). In this , the pixels covered by these five classes of regolith are shown in the Table-I.

Slope

As the slope is one of the vital parameters controlling the landslides, the slope map of the study area was prepared classifying the area into 4 classes of slopes viz. steep, moderate, shallow, and rolling slopes, based on the amount of inclination i.e., the zones having more than 40° slope were marked as steep, 40° - 20° as moderate, 20°- 3° as shallow and less than 3° as rolling slopes. To map such various slopes, the Survey of India Topographic sheet of 1:50,000 scale having 20-meter contours was enlarged to 1:12,500 scale and then by measuring the distance between the two adjacent 20-meter contours, various slope classes were mapped. For example, if the distance between the two contours was less than 2mm, the said zone was mapped as steep slope, 2mm - 4.4mm as moderate, 4.4mm to 28mm as shallow and more than 28mm as rolling slopes. Such slope classes mapped in vector GIS layer was converted into raster GIS layer using ArcGIS with the same pixel size of 23.5x23.5 m² used for the other geosystem variables. In it, the steep slopes occupied 50,464 pixels, moderate had 1,03,787 Pixels, shallow had 3,90,422 pixels and the rolling slopes covered 7,784 pixels in the overall pixels of 5,52,456 of the study area (Fig. 3I).

Geomorphology

Geomorphology is another major important geosystem variable having direct and significant control over the landslides. This is so, because the geomorphology/landforms are the resultant product of palaeo, time transgressive and the ongoing geological processes and further, the ultimate disaster vulnerability of the terrain also depends upon the geomorphology. So, GIS database was generated on the geomorphology of the study area by interpreting various geomorphic features viz. Escarpments, Tor Cliffs, Mid Slope Mounds, Barren Rocky Slopes, Slopes with Settlements, and the other landforms numbering over 12 shown in figure 4A. This was prepared by interpreting IRS P6 LISS III FCC data and the same wrapped over SRTM Digital Elevation Model. Such geomorphology map prepared as vector GIS data was converted into raster GIS data with same pixel size and the same total numbers of pixels for the study area as was done in the case other geosystem parameters (Fig.4A).In this , the number of pixels covered by these twelve geomorphic sub variables are shown in Table-I.

Land Use / Land Cover

The IRS P6 LISS III FCC data was digitally zoomed to 1:10,000 scale in Arc GIS and Landuse / Land Cover features were interpreted. Viz. Reserve Forests, Dense Forests, Scrub Forests, Open Forests, Forest blanks and the other features numbering over 10 sub variables/ features. In addition to FCC data, where ever required, different types of image processing techniques like classification and pseudo color composites generated from principal component images were also used. Such LU/LC map was also converted into a raster GIS layer with same pixel size of 23.5X23.5 m² and same total number of pixels of 5,52,456 for the study area matching with other geosystem variables (Fig.4B).

Drainage Density

The study area had prolific development of drainages and deeply dissected the area. Further as these drainages have significant control over the landslides, the vector GIS database was generated on the drainage density. This was accomplished by drawing the drainages of the study area from the aerial photographs of 1:10,000 scale, recent satellite images and the topographic sheets. Then the drainage density map was prepared by counting the total length of drainages per 250 x250 m² grid, plotting them in the respective grid centres and contouring them using surfer software. The drainage density so derived for the study area varied from 0 to 400m per grid. This was grouped into 5 categories (viz, >300m - Very High, 300 to 200 - High, 200 to 100 - Moderate, 100 to 1 - Low and < 1m - Very Low and raster GIS data was generated (Fig 4C). The number of pixels occupied by these five classes of slopes are shown in Table-I.

Landslide Vulnerability Mapping

Calculation of Information Value for Sub Variables

Subsequent to the generation of raster GIS data bases on the above various 12 geosystem parameters/ main variables , the information values were worked out for each sub variable of these 12 geosystem variables(Figs -3 &4) , integrated together and landslide vulnerability map was prepared as briefed in the methodology section above and also as detailed below:-

$$\text{Information value} = \log (S_i/N_i) / (S/N)$$

Where,

(i) S_i = Number of Landslide pixels falling in a particular sub variable (say, lithology)

(ii) N_i = Total number of pixels covered by the said sub variable of the lithology main variable

(iii) S = Total number of landslide pixels of the study area

(iv) N = Total number of pixels of the study area.

For example, the three sub variables of Lithology raster data namely highly, moderately and poorly weathered Charnockites respectively had 2,17,983; 2,07,817 and 1,26,656 pixels. The information values were worked out for each such sub variable by superimposing the raster GIS data on landslides over the raster GIS data on lithology. For example, the IFOV (Information Value) worked out for the highly weathered Charnockite will be as follows. (i) Totally 100 number of landslides pixels were falling in highly weathered Charnockite; so the same value of 100 was taken as 'Si' value and (ii) the total number of pixels of 2,17,983 covered by the highly weathered Charnockite was taken as 'Ni' value. (iii) Whereas the total number of landslide pixels of 144 of the study area were taken as 'S' values and the(iv) total number of 5,52,456 pixels of the entire study area were considered as 'N' value. Then, by substituting these values in the formula, the information value was worked out for the sub variable highly weathered Charnockite of the main lithology variable Charnockite as follows: -

$$\text{Information value of highly weathered Charnockite} = \log (S_i/N_i) / (S/N)$$

$$= [\log (100/2,17,983)/ (144/5,52,456)]$$

$$= 0.245$$

The information value of 0.245 thus workout for the highly weathered Charnockite was assigned to all the 2,17,983 pixels of the sub variable ,the highly weathered Charnockites. Similarly the information values were worked out for the other two sub variables of Charnockite, namely the moderately weathered and the poorly weathered Charnockites and these IFOV values were accordingly assigned to the respective pixels of these two sub variables. In the same way, the information values were worked out for all the sub variables of all the other 11 geosystem variables. The information values worked out thus for the sub variables of the 12 main variables are shown in the following Table-1 and shown in brackets against each of the geosystem parameter in Figs -3 and 4. Thus, each pixel of the each sub variables had their IFOV weightages.

Table 1: Information value based Landslide Vulnerability weightages

Sl. No	Class/ Subvariables of geosystems	Si	Ni	S	N	(Si/Ni) / (S/N)	Infor. Value Log (Si/Ni) / (S/N)
Lithology							
1	Highly Weathered Charnockite	100	217983	144	552456	1.76	0.245
2	Moderately Weathered Charnockite	12	207817			0.222	-0.654
3	Poorly Weathered Charnockite	32	126656			0.997	-0.001
Lineament Frequency							
1	Very High	0	2306	144	552456	0	0
2	High	9	30231			1.142	0.133
3	Moderate	52	178843			1.115	0.109
4	Low	83	295008			1.079	0.076
5	Very Low	0	46068			0	0
Lineament Density							
1	Very High	19	69170	144	552456	1.054	0.023
2	High	25	104012			0.922	-0.035
3	Moderate	47	175025			1.03	0.013
4	Low	53	154278			1.318	0.12
5	Very Low	0	49971			0	0
Lineament Intersection Density							
1	Very High	0	1858	144	552456	0	0
2	High	14	22779			2.358	0.372
3	Moderate	58	294585			0.755	-0.12
4	Low	72	204686			1.35	0.13
5	Very Low	0	28548			0	0
Azimuths between topographic Ridges and Joints in degrees							
1	<5	16	37006	144	552456	1.659	0.22

2	10-May	2	20085			0.382	-0.418
3	20-Oct	29	93712			1.187	0.075
4	20-30	26	76359			1.306	0.116
5	>30	71	325294			0.837	-0.077
Angle between slope of the topographic ridges and dip of joints in degrees							
1	>-10	118	436366	144	552456	1.037	0.016
2	(-10) - (0)	12	44798			1.028	0.012
3	0	4	2730			5.621	0.75
4	0-10	3	27530			0.418	-0.379
5	>10	7	41032			0.655	-0.184
Dip Amount of Joints in degrees							
1	<15	8	40873	144	552456	0.751	-0.124
2	15 - 25	12	16256			2.832	0.452
3	25-35	11	44727			0.944	-0.025
4	35-45	5	46270			0.415	-0.382
5	>45	108	404330			1.025	0.011
Regolith							
1	> 35	22	70124	144	552456	1.2	0.08
2	25 -35	56	193990			1.11	0.04
3	15 -25	55	209723			1.01	0
4	15-May	10	70497			0.54	-0.26
5	< 5	1	8122			0.47	-0.33
Slope							
1	Steep	22	50464	144	552456	1.673	0.223
2	Moderate	77	103782			2.846	0.454
3	Shallow	45	390422			0.442	-0.354
4	Rolling	0	7788			0	0
Geomorphology							
1	Escarpment	4	3130	144	552456	4.9	0.69
2	Tor Cliff	4	995			15.42	1.19
3	Mid Slope Mound	3	3536			3.25	0.51
4	Barren Rocky Slopes	20	20605			3.72	0.57
5	Slopes With Settlements	31	25542			4.66	0.67
6	Slopes With Plantations	44	260554			0.65	-0.19
7	Slopes With Natural Vegetations	27	152043			0.68	-0.17
8	Filled Valleys	2	56619			0.14	-0.87
9	Filled Fracture Valley	3	11760			0.98	-0.01

10	Barren Valley	5	11923			1.61	0.21
11	Barren Fracture Valley	1	2718			1.41	0.15
12	Water Body	0	3031			0	0
Landuse / Land Cover							
1	Reserve Forest	10	33177	144	552456	6.94	0.06
2	Dense Forest	29	136307			20.14	-0.09
3	Scrub Forest	3	8436			2.08	0.14
4	Open Forest	5	25468			3.47	-0.12
5	Forest Blank	31	67720			21.53	0.24
6	Plantation	59	255695			40.97	-0.05
7	Open Plantation	0	2382			0	0
8	Settlement	7	18617			4.86	0.16
9	Water Logged Areas	0	3631			0	0
10	Water Body	0	1023			0	0
Drainage Density							
1	>300	0	31	144	552456	0	0
2	200-300	17	81841			0.8	-0.1
3	100-200	86	325759			1.01	0.01
4	0-100	30	127542			0.9	-0.05
5	0	11	17283			2.44	0.39

GIS Integration of Weighted Geosystem Layers and Landslide Vulnerability Mapping

After the generation of such information value based weighted GIS raster layers for the above 12 geosystem layers/variables, all the 12 were integrated together using the Raster calculator menu of the Spatial Analyst extension module of the Arc GIS. In this process, the information value of each pixel of each layer was added with corresponding pixel of all the 12 geosystem layers / variables and thus the 5,54,456 pixels of the integrated GIS layer had accrued the total weightages of all the 12 layers which ranged from -2.81 to 2.67, as shown in figure 6. The dynamic range of cumulative information values from -2.81 to 2.67 of the 5,54,456 pixels were rescaled from 0 to 10. Then based on the rescaled IFOV values the area was regrouped in to 5 classes of landslide vulnerability viz: 0-1.9 as Very Low, 2 – 3.9 as Low, 4 – 5.9 as moderate, 6- 7.9 as High and 8 – 10 as Very high and such regrouped pixels of the 5 classes and the landslide vulnerability are shown in figure 7.

Validation and Conclusion

For Validating this method of landslide vulnerability mapping, landslide incidence map of the study area(Fig-1) was superimposed over the final Landslide Vulnerability Map(Fig-7) which revealed that out of 144 landslides, 94 landslides (65%) fell in Very High and Highly vulnerable zones, 47 in Moderate (33%) and 3 in Low (2%) vulnerable zones indicating that this method has yielded fairly precise landslide vulnerability map. However, efficiency of this method depends on the fact that maximum landslides must fall in minimum area in each identified very high and highly vulnerable zones. To evaluate this, landslides per unit area (LS/A) was worked out, which indicated that LS/A was 13.88 in very highly vulnerable zone and 2.89 in highly vulnerable zone and least in other cases (Table 2). This indicates that the information value method is an efficient method and can produce precise information on landslide vulnerability mapping. Now these very highly and highly vulnerable zones are the sen-

sitive hotspots and even minor triggering by way of toe removal, deforestation, rainfall etc. can cause landslides.

This method can be successfully replicated in other regions of the world following the methodology described in the article. But the constraint is that the region of study should have enough and broad distribution of landslide locations .Several methods like GIS based slope ,integrated terrain , Weight of evidence ,Index overlay and Bureau of Indian Standard methods have been used [28] and among which the present Information value method seems to have given greater precision in land slide vulnerability mapping as seen from the validation in the study. In this study, the major mappable human interventions in the area like deforestation, open forest caused by the human beings and the plantations cultivated by the human beings by removing the forest areas have been taken as sub variables in the land use /cover map and weightages were assigned to them . So, all these significantly add credibility to this method. Again as far as the risk management and mitigation strategies are concerned , the management plans in the very high and highly vulnerable areas can be done in the form afforestation , gully plugging, check damming, protection walling with weep holes and other similar measures depending upon the terrain conditions .

Table 2: Landslide Vulnerability Zones

Sl. No.	Landslide Vulnerability Zones	LS	Area coverage (Sq.Km) (A)	LS / A
1	Very High	15	1.08	13.88
2	High	79	27.29	2.89
3	Moderate	47	146.01	0.321
4	Low	3	111.85	0.026
5	Very Low	0	10.76	0
	Total	144	297	0.485

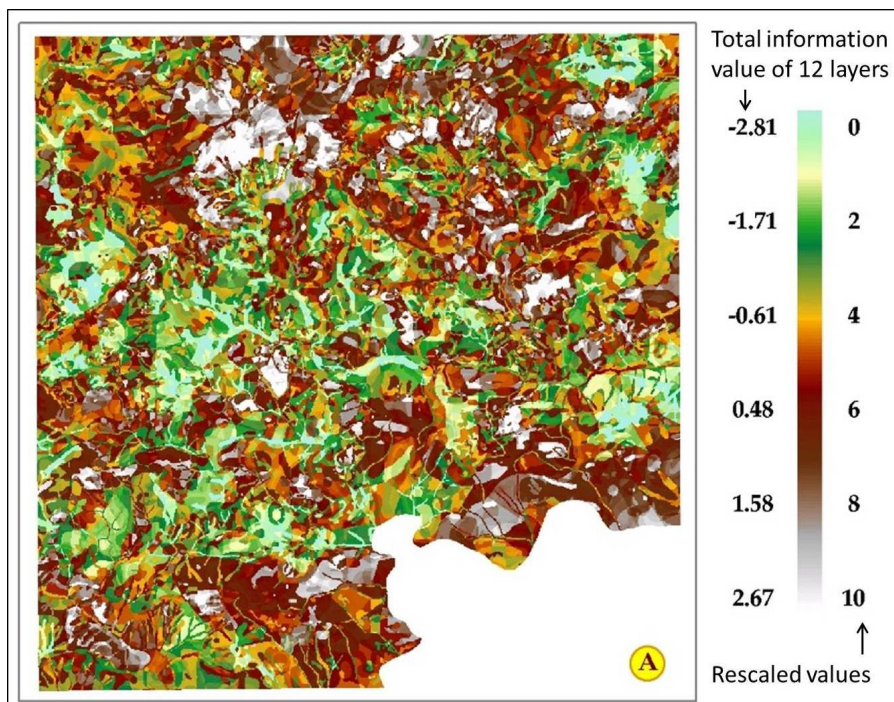


Figure 6: Integrated GIS output having the cumulative information values of all the 12 geosystem variable

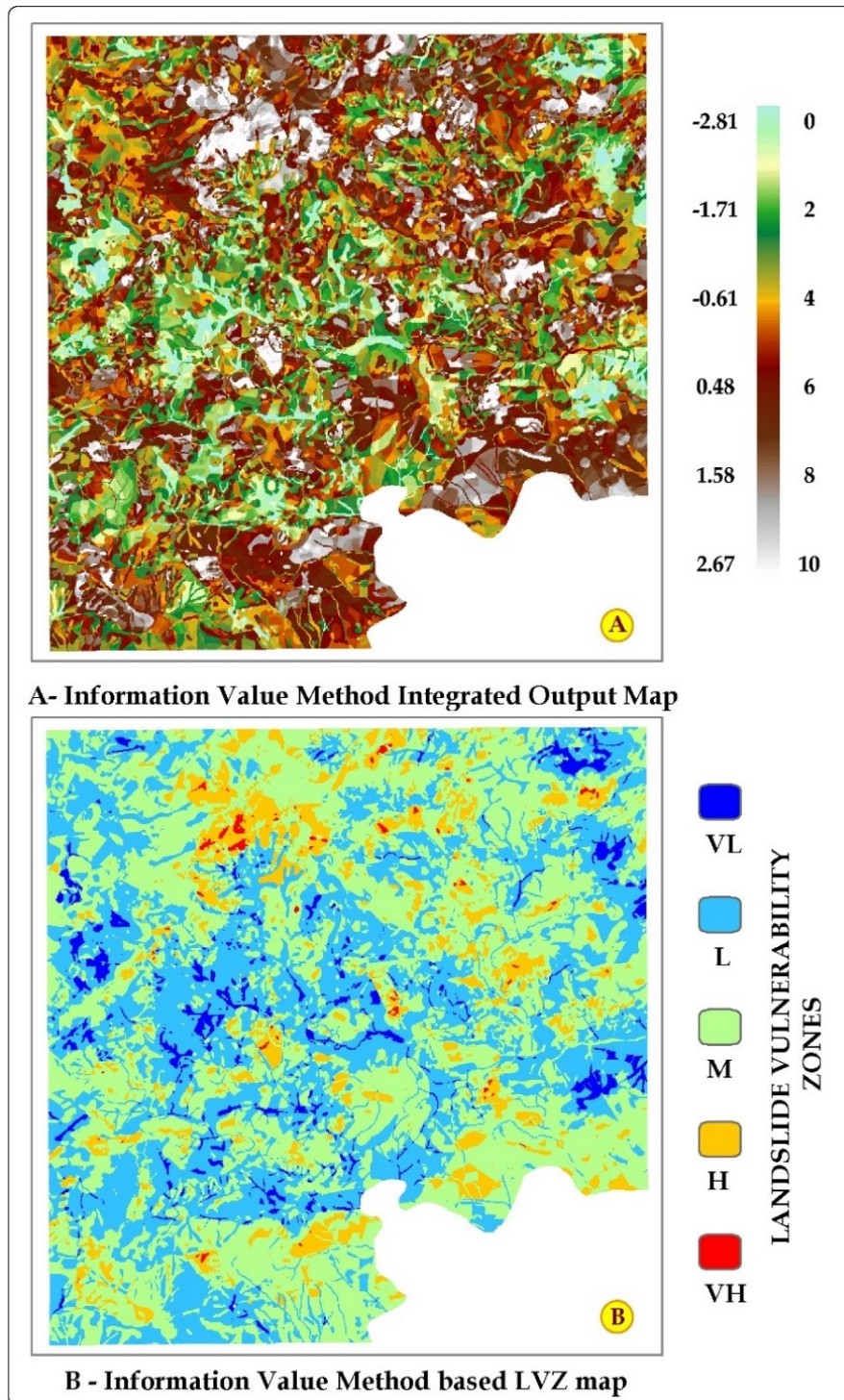


Figure 7: Information value based Landslide vulnerability Map

Acknowledgement

The senior author acknowledges the Dept of Science and Technology , Govt of India , New Delhi for having funded the research project to him and the junior author acknowledges for having provided JRF/Scientist position to work on the project . The Bharathidasan university is also acknowledged

References

1. Didwal RS (1980) Occurrence of Landslides in Jammu Province of J and K state and their control", *Proceedings, International Symposium on Landslides*, (ISL 1980), April 7-11, New Delhi, 1: 37-40.
2. Rodríguez CE, Bommer JJ Chandlerand RJ (1999) Earthquake-induced landslides: 1980–1997. *Soil Dynamics and Earthquake Engineering* 18: 325-46.
3. Chi-Ming Yang, Jan-Chang Chen, Lan-Lin Peng, Jr-Syu Yang, Chang-Hung Chou (2002) Chi-Chi Earthquake-caused Landslide: grey prediction model for pioneer vegetation recovery monitored by satellite images. *Bot.Bull.Acad.Sim*, 43: 69-75.
4. Pradhan B, Singh RP, Buchroithner MF (2006) Estimation of stress and its use in evaluation of landslide prone regions using remote sensing data. *Advances in Space Research*, 37: 698-709.
5. Arun Kumar, Anderson, UmangKapoor, Sunil Dhar, Chingkhei RK (2008) Landslide Hazard Zonation Atlas of Northeast India. *Indian Landslides*, 1: 11-18.
6. Xu C, Shyu, J BH, Xu X (2014) Landslides triggered by the 12 January 2010 Port-au-Prince, Haiti, Mw = 7.0 earthquakes: visual interpretation, inventory compiling, and spatial distribution statistical analysis. *Nat. Hazards Earth Syst. Sci*, 14: 1789-818.
7. Ramasamy SM, Muthukumar M, Subagunasekar M (2015) Malin-Maharashtra landslides: a disaster triggered by tectonics and anthropogenic phenomena. *Current Sciences*, 108: 1428-30.
8. Gutierrez F, Zarei M, Hudec MR, Deirnik H (2023) Normal faulting and landsliding in morpho-structural domes related to buried salt stocks, Zagros Mountains, Iran. Insights into salt breakout. *Marine and Petroleum Geology*, 106376.
9. Seshagiri DN, Badrinarayanan S, Upendran R, Lakshminathan CB, Srinivasan V (1982) The Nilgiri Landslides. Geological Survey of India. *Miscellaneous publications*, 57: 41.
10. Pachauri AK, Pant M (1992) Landslide hazard mapping based on geological attributes. *Engineering Geology*, 32: 81-100.
11. Wasowki J (1998) Understanding rainfall-landslide relationships in man modified environments: A case history from Carmanico Terme, Italy. *Environ. Geol*, 35 : 197-209.
12. Moeyersonsa J, Ph Trefois, J Lavreau, D Alimasi, I Badriyo, (2004) A geomorphological assessment of landslide origin at Bukavu, Democratic Republic of the Congo, *Engineering Geology*, 72: 73-87.
13. Kuriakose, S Lillisand, Sankar GE, Muraleedharan C (2009) History of landslide susceptibility and a chorology of landslide-prone areas in the Western Ghats of Kerala, India. *Environ Geol*, 57: 553-1568
14. Galeandro A, Simon V (2012) Infiltration processes in fractured and swelling soils and their influence on the stability of surficial covers. *Rendiconti Online della Societa`Geologica Italiana*, 2: 518-20
15. Calderon-Aguilera Luis E, Victor H Rivera-Monroy, Luciana Porter-Bolland, Angelina Martinez-Yrizar, Lydia B Ladah, et al. (2012) An assessment of natural and human disturbance effects on Mexican ecosystems: current trends and research gaps. *Biodivers Conserv*, 21: 589-617.
16. Havenith HB, Torgoev A, Braun A, Schlögel R, Micu M (2016) A new classification of earthquake-induced landslide event sizes based on seismotectonic, topographic, climatic and geologic factors. *Geoenvironmental Disasters*, 3: 1-24.

17. Gill JC, Bruce D, Malamud (2017) Anthropogenic processes, natural hazards, and interactions in a multi-hazard framework. *Earth-Science Reviews*, 166: 246-69.
18. Reyes-Carmona C, Galve JP, Pérez-Peña JV, Moreno-Sánchez M, Alfonso-Jord D, et al. (2023) Improving landslide inventories by combining satellite interferometry and landscape analysis: the case of Sierra Nevada (Southern Spain). *Landslides*, 1-21.
19. Brenning A (2005) Spatial prediction models for landslide hazards: review comparison and evaluation. *Natural Hazards and Earth System Sciences*, 5: 853-62.
20. Francisco Gutiérrez, Mauro Soldati, Franck Audemard, Dan Bălteanu (2010) Recent advances in landslide investigation: Issues and perspectives. *Geomorphology*, 124: 95-101.
21. Moses Musinguzi, Immaculate Asimwe (2014) Application of Geospatial Tools for Landslide Hazard Assessment for Uganda. *South African Journal of Geomatics*, 3: 302-14.
22. Ebrahim Karimi Sangchini, Mohammad Reza Nowjavan, Abdolhossein Arami (2015) Landslide susceptibility mapping using logistic statistical regression in Babaheydar Watershed, Chaharmahal Va Bakhtiari Province, Iran. *Journal of the Faculty of Forestry Istanbul University*, 65 : 30-40.
23. Himan Shahabi, Mazlan Hashim (2015) Landslide susceptibility mapping using GIS-based statistical models and Remote sensing data in tropical environment. *Scientific reports* 5: 9899.
24. Mandal B, Mondal S, Mandal S (2023) GIS-based landslide susceptibility zonation (LSZ) mapping of Darjeeling Himalaya, India using weights of evidence (WoE) model. *Arabian Journal of Geosciences*, 16: 1-20.
25. Ramasamy (1995) lineament analysis and stress modeling of Vindhyan Basin, Rajasthan, india. *Mem. Geological society of India*, 31: 279-310.
26. Yin KL, Yan TZ (1988) Statistical prediction model for slope instability of metamorphosed rocks. *In Proceedings of the 5th international symposium on landslides, Lausanne, Switzerland*, 2: 1269-72.
27. Muthukumar M (2009) Geomatics based optimum landslide vulnerability mapping model-Nilgiri mountains, South India. Thesis submitted for Doctor of philosophy in geological remote sensing, Bharathidasan university , Tiruchirappalli, India, unpublished, 187.